A Transfer Standard for Measuring Photoreceiver Frequency Response

Paul D. Hale, C. M. Wang, Rin Park, and Wai Yuen Lau

Abstract— **We have developed a photoreceiver frequency response transfer standard which can be used to measure the optical modulation transfer function of a modulated optical source. It combines a photodiode with an RF power sensor or an amplified receiver with an RF power sensor. It is calibrated with an expanded uncertainty of 0.06 dB (coverage factor = 2) using a heterodyne technique at 1.319 μm. We present a theory which allows use of the transfer standard with arbitrary source modulation depth. The calibration is transferred to a SDH/SONET test equipment manufacturer giving a final uncertainty well below the 0.3 dB uncertainty specified by ITU-TS (formerly CCITT) recommendation G.957. The transfer standard may have other applications including calibration of CATV test equipment, lightwave component analyzers, and lightwave spectrum analyzers.**

I. Introduction

INCREASED commercial availability of optoelectronic devices and test equipment requires the availability of accurate low-cost optoelectronic frequency response calibrations which are traceable to national standards. Examples of this need are the SDH/SONET (synchronous digital hierarchy/synchronous optical network) standard test receiver, which is specified [2] as having a fourth-order Bessel–Thompson filter response with tolerances [3], [4] as low as ±0.3 dB or instrumentation for CATV which has comparable tolerances. Until recently, uncertainties this low were not possible [5], [6]. Transfer standard receivers which are calibrated by a standards laboratory must have uncertainties which are at least a factor of 4 smaller.

In the past, photoreceiver frequency response measurements have had high uncertainties for two reasons: inaccurate knowledge of the optical stimulus and large uncertainties in the microwave power calibration. With careful attention to system performance, uncertainties around 0.12 dB to 0.45 dB can be achieved [5]. This accuracy is not adequate to support the ±0.3 dB SDH/SONET tolerance specifications with adequate confidence.

In a well-designed heterodyne measurement system the uncertainty in optical stimulus can be reduced to ±0.0023 dB (1σ). Typical RF power sensor calibration uncertainties are about a factor of 15 or 20 higher (for 1σ). Uncertainties due to mismatch can be 0.1 dB or higher. Mismatch errors can be corrected, but it is unclear that the uncertainty in the corrections is low enough to give adequately improved uncertainty. If the uncertainty due to RF calibration and impedance mismatch could be eliminated, the overall optoelectronic response uncertainty could be significantly reduced. In this work we describe a method for calibrating a photoreceiver frequency response transfer standard with the low inherent uncertainty of the NIST Nd:YAG heterodyne system. This is achieved by combining a photoreceiver with a microwave power sensor and calibrating the response of the combined unit, eliminating RF calibration and mismatch uncertainties. The theory for measuring an unknown device against the transfer standard is also derived. This transfer standard is then used to calibrate the optical modulation transfer function of a customers test system while maintaining a low uncertainty. Uncertainty in the customers measurement is further reduced when the device under test combines an optical-to-electrical converter and a power measurement device. This is the case for the system for calibrating lightwave communications analyzers which is described.

Special examples of two transfer standards will be used throughout this work. These transfer standards were chosen as representative of the types of photoreceivers which would be used in the factory for testing SDH/SONET, CATV, and lightwave component analyzer frequency response. The first is a dc-coupled photodiode combined with a 3 dB attenuator and a diode-based microwave power sensor. The photodiode is equipped with a bias current monitor circuit (monitored externally), has about 0.7 A/W responsivity at dc, and has a 20 GHz nominal optical bandwidth. The second example is a packaged photodiode with a dc-coupled transimpedance amplifier. This device does not give external access to the photocurrent. It has a conversion factor of about 700 V/W at dc and 1 GHz optical bandwidth. The receiver is combined with a thermocouple-based microwave power sensor.

II. Nd:YAG Heterodyne Measurement System

NIST uses a Nd:YAG heterodyne system for measuring scalar frequency response because the excitation of the detector can be calculated from first principles. All system calibrations required are well understood and independent of the frequency response measurement. A schematic of the heterodyne system is shown in Fig. 1. The system uses two commercially available single-mode monolithic-ring Nd:YAG lasers operating at 1.319 μm. The frequency of each laser can be tuned thermally to give beat frequencies from several tens of kilohertz to greater than 50 GHz; the beats have a

Manuscript received March 14, 1996; revised July 31, 1996.

P. D. Hale is with the Optoelectronics Division, National Institute of Standards and Technology, Boulder, CO 80303 USA.

C. M. Wang is with the Statistical Engineering Division, National Institute of Standards and Technology, Boulder, CO 80303 USA.

R. Park and W. Y. Lau are with the Lightwave Operation, Hewlett-Packard Company, Santa Rosa, CA 95403 USA.

Publisher Item Identifier S 0733-8724(96)08752-X.

0733–8724/96$05.00 © 1996 IEEE

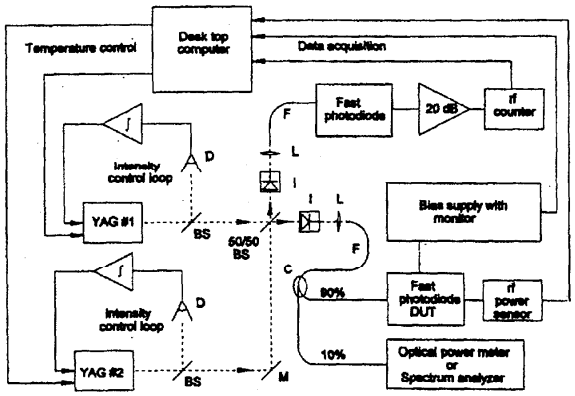

Fig. 1. NIST Nd:YAG heterodyne system. Labeled components are beam splitter (BS), mirror (M), isolator (I), lens (L), single-mode fiber (F), large area detector (D), and integrating amplifier ($\int$).

short-term bandwidth of less than 3 kHz. The beat frequency is measured with a microwave counter. As the frequency is scanned, data are acquired automatically. The resolution of the system is limited by the scan rate, the frequency jitter, and the time constants of the data acquisition equipment. At present, the highest resolution achievable is about 200 kHz, although resolution may be considerably worse when the frequency is swept quickly (for example, when a much larger data spacing is desired).

The repeatability is greatly degraded when crossing through dc because of the frequency jitter of the lasers, the relatively slow response of the power meter, and steep 100 kHz cutoff of the power sensor. As the frequency is swept through dc, the RF power drops to 0 and the power meter cannot track this drop even if the sweep speed is greatly reduced. The lowest frequency where good repeatability is achieved is around 200 kHz when a sensor with 100 kHz cutoff is used. Also, when the frequency passes through dc, the dc photocurrent is indeterminate because the phase relationship between the two lasers is arbitrary and the frequency drift is small (but significant) over one time constant of the equipment. This problem has recently been overcome using a phase-locked loop technique and will be described in a later paper. Repeatability is not a problem near the cutoff of a 50 MHz cutoff power sensor.

The lasers are power stabilized so that nearly equal power from each laser is delivered to the DUT (device under test). The combined laser beams pass through polarizing isolators so that the signal from each laser is in the same polarization state when it reaches the DUT; this ensures nearly 100% modulation depth and eliminates instabilities due to feedback. Effects of fiber or other component birefringence after the isolators are insignificant. The total optical power incident on the photoreceiver is

$$P_{\text{total}}(t) = (P_{O1} + P_{O2}) + 2\sqrt{P_{O1}P_{O2}}\cos(2\pi f t) \quad (1)$$

where P_{O1} and P_{O2} are the optical powers delivered to the photoreceiver from the lasers, f is the difference frequency between the two lasers, and t is time.

III. Photodiode with Access to Bias Monitor

The photocurrent generated by the photodiode is given by

$$\begin{aligned} i_p(f,t) &= (P_{O1} + P_{O2})R(0) + 2\sqrt{P_{O1}P_{O2}}R(f) \\ &\quad \cdot \cos(2\pi f t + \phi(f)) \\ &= i_{\text{dc}} + i_{\text{RF}} \end{aligned} \quad (2)$$

where $R(f)$ is the responsivity of the detector (in A/W) at frequency f and $\phi(f)$ accounts for phase delay in the photodiode, transmission line, and connectors. For the purposes of this paper phase will be neglected. The first term on the right side is the dc photocurrent, which flows through the bias supply, and the second term is the RF photocurrent which flows through the RF load (the microwave power sensor) through a dc blocking capacitor. The mean squared photocurrent generated by the photodiode is

$$\begin{aligned} \langle i_p^2(f)\rangle &= (P_{O1} + P_{O2})^2R^2(0) + 2P_{O1}P_{O2}R^2(f) \\ &= \langle i_{\text{dc}}^2\rangle + \langle i_{\text{RF}}^2\rangle. \end{aligned} \quad (3)$$

If P_{O1} is nearly equal to P_{O2}, then $2(P_{O1}P_{O2})$ is, to first order, equal to $0.5(P_{O1} + P_{O2})^2$. The normalized frequency response, $\Re^2$, which is defined as $R^2(f)/R^2(0)$, can then be found by taking the ratio of the RF power to the dc electrical power delivered to a load R_L

$$\begin{aligned} \frac{2P_{\text{RF}}}{\langle i_{\text{dc}}^2\rangle R_L} &= \frac{\langle i_{\text{RF}}^2\rangle R_L}{0.5\langle i_{\text{dc}}^2\rangle R_L} \\ &= \frac{2(P_{O1}P_{O2})R^2(f)R_L}{0.5(P_{O1} + P_{O2})^2R^2(0)R_L} \\ &\approx \frac{R^2(f)}{R^2(0)} \\ &\equiv \Re^2(f). \end{aligned} \quad (4)$$

P_{RF} is a function of frequency. It includes corrections for sensor calibration factor and mismatch, and is the power that would be delivered to an ideal load R_L [7]. Our measurements were made with transmission lines and loads with characteristic impedance of 50 Ω; however, these equations also apply to measurements with 75 Ω systems. The normalized frequency response may be quoted in decibels as $20\log[\Re(f)]$. The electrical bandwidth of the device is where $20\log[\Re(f)]$ falls by 3 dB from the low frequency level [3].

In an ideal measurement $\langle i_{\text{dc}}^2\rangle$ is constant, but in any real measurement system it may vary because of changing optical power coupled to the photodiode. Using the normalized response simplifies the measurement because only the total photocurrent in the DUT need be monitored instead of the power coupled to the detector from each laser. The ratio in (4) is insensitive to optical power variations. Accuracy is increased by reducing the effect of power variations due to Fresnel reflections at poorly terminated fiber ends (including the ends of couplers which are used as power monitors and connector-to-connector interfaces). The absolute RF responsivity is calculated by multiplying the normalized frequency response by the square of the dc responsivity which is measured separately. Because most fast commercial photodetector packages are pigtailed and connectorized, the uncertainty of the absolute

responsivity includes the uncertainty of the fiber connector insertion loss. Variations in connector insertion loss may be high and can contribute to significant uncertainties in the absolute response [8], [9]. A correction must be made for these variations to attain the desired uncertainty. This problem will be discussed further in the section on uncertainty analysis for the amplified photoreceiver, below.

IV. Photoreceiver with No Access to Bias Monitor

For some applications it is desirable to know the absolute voltage response of the photoreceiver. An amplified photoreceiver commonly requires this type of characterization. For a photoreceiver without a bias current monitor, the system in Fig. 1 includes a 10 dB (nominal) optical coupler which monitors the total power from the lasers during a frequency scan. The power incident on the DUT is inferred from the coupler monitor port. The voltage which the receiver delivers to a load RL is given by

$$V_p(f,t) = (P_{O1} + P_{O2})G(0) + 2\sqrt{P_{O1}P_{O2}}G(f) \cdot \cos(2\pi f t) \tag{5}$$

where $G(f)$ is the amplified response of the detector (in V/W) at frequency f. The first term on the right side is the average dc signal, and the second term is the RF signal. The voltage response is found in a similar manner to (3) and (4) and is

$$G^2(f) = \frac{2R_L P_{\mathrm{RF}}}{P_{\mathrm{avg}}^2} \tag{6}$$

where $P_{\mathrm{avg}} = P_{O1} + P_{O2}$ is the average (dc) optical power incident on the detector and P_{RF} is the electrical power delivered to a load R_L (the power sensor). This ratio is insensitive to small changes in power from either laser because the powers from the two lasers are nearly equal. If the voltage response is measured in dB (1 V/W), $R_L = 50\,\Omega$, RF power in dB (1 mW), and the average optical power is in dB (1 mW), (6) can be written as [2]

$$20\log(G(f)) = 50 + \wp_{\mathrm{RF}} - 2\wp_{\mathrm{avg}} \tag{7}$$

where $\wp$ denotes a power measured in dB (1 mW).

V. Application of Formalism to Arbitrary Modulation Depth

Signals which do not have 100% modulation depth are commonly used in optoelectronic test equipment. An arbitrary modulation depth can be synthesized by varying one or both of the laser powers in the heterodyne system and can be modeled using the same formalism as above. The resulting equations are applicable to any source with an arbitrary modulation depth, such as a laser with direct or external modulation. A notationally simple way to change the model is to let $P_{O1} = \alpha P_O$ and $P_{O2} = (1-\alpha)P_O$. Then the total optical signal incident on the photodiode is

$$P_{\mathrm{total}}(t) = P_O + 2P_O\sqrt{\alpha(1-\alpha)}\cos(2\pi f t). \tag{8}$$

The average optical power is then P_O and the absolute modulation depth is $4P_O[\alpha(1-\alpha)]^{1/2}$, or, in fractional units the fractional modulation depth M_O is

$$M_O = \frac{P_{\max} - P_{\min}}{2P_O} = 2\sqrt{\alpha(1-\alpha)} \tag{9}$$

where $P_{\max}$ and $P_{\min}$ are the maximum and minimum optical powers incident on the receiver. The mean squared currents in the photodiode are

$$\langle i_{\mathrm{dc}}^2 \rangle = P_O^2 R^2(0) \tag{10}$$

and

$$\langle i_{\mathrm{RF}}^2 \rangle = 2P_O^2\alpha(1-\alpha)R^2(\omega) \tag{11}$$

so the ratio of the powers is

$$\frac{2P_{\mathrm{RF}}}{\langle i_{\mathrm{dc}}^2 \rangle R_L} = M_O^2 \Re^2(f). \tag{12}$$

Hence, the modulation depth of an arbitrary source can be measured with a detector of known normalized response.

In the case of the amplified receiver, the modulation depth of an unknown source can be found in terms of the measured RF power, average optical power, and known voltage frequency response as

$$M_O^2 = \frac{2R_L P_{\mathrm{RF}}}{G^2(f)P_{\mathrm{avg}}^2}. \tag{13}$$

VI. Calibration Transfer Using Ratio of Measurements

The fundamental problem in making photodetector frequency response measurements is getting accurate knowledge of the modulation depth of the source. The modulation depth of the heterodyne beat signal is known from fundamental principles, but the modulation depth of a directly modulated laser diode is not. The modulation depth of a Mach–Zehnder modulator can be measured, but careful control of bias and net optical transmission are required for accurate measurements. A transfer standard calibrated using the heterodyne techniques described above and the ratio measurement system shown in Fig. 2 can be used to obtain accurate knowledge of the modulation depth of these sources. The ratio system consists of a modulated light source with unknown modulation depth and a 1×2 coupler. The coupling ratio does not need to be specified. The signal from the coupler is delivered to a DUT and to a reference photodiode attached to a RF power sensor. The modulation depth of the source can be calculated using (12) and the known frequency response of the transfer standard photodiode. Then the frequency response of the DUT is

$$\Re_{\mathrm{DUT}}^2(f) = \left[\frac{1}{M_O^2}\right]\frac{P_{\mathrm{RF:DUT}}}{0.5\langle i_{\mathrm{dc:DUT}}^2 \rangle R_L}. \tag{14}$$

Calculation of the DUT's frequency response this way includes calibration uncertainty of both the power sensors used to measure P_{RF} from the standard detector at NIST and at the customers laboratory, giving a total expanded uncertainty of ± 0.2 dB or more for the modulation transfer function. Combined with other factory uncertainties, this may give an unacceptable uncertainty for the intended test system.

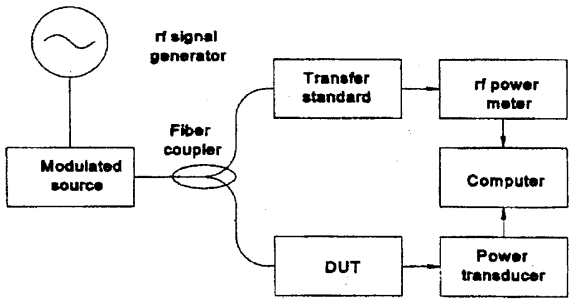

Fig. 2. Apparatus for measuring modulation depth of unknown source to calibrate DUT. Power transducer may be internal or external to DUT.

One possible alternative is to calibrate the response of the photodiode combined with the RF power sensor. This method totally eliminates uncertainties due to power sensor calibration and impedance mismatch. The combined frequency response $\mathbb{R}^2(f)$ measured on the NIST heterodyne measurement system includes the power sensor calibration factor and impedance mismatch, and is given by

$$\mathbb{R}^2(f) = \frac{\Re^2(f)}{C} = \frac{P_m}{0.5\langle i_{\rm dc}^2\rangle R_L}. \tag{15}$$

In (15), P_m is the indication of the power meter after zeroing and calibration against the 50 MHz reference signal (from the power meter) using a calibration factor of 100%. C is given by

$$C = \frac{1}{k}|1 - \Gamma_{\rm pd}\Gamma_{\rm sensor}|^2 \tag{16}$$

where k is the sensor calibration factor and $\Gamma_{\rm pd}$ and $\Gamma_{\rm sensor}$ are complex reflection coefficients. However, C does not need to be known and the power meter reading does not need to be corrected with a frequency dependant calibration factor. When the photodiode/power sensor combination transfer standard is used in the ratio test system the combined frequency response is used to find the modulation depth of the source

$$M_O^2 = \left[\frac{1}{\mathbb{R}^2(f)}\right]\frac{P_{m:\rm ref}}{0.5\langle i_{\rm dc:ref}^2\rangle R_L}. \tag{17}$$

The normalized response of the DUT is then found using (17), the dc photocurrent, and the RF power (including all calibration factors) from the DUT

$$\Re_{\rm DUT}^2(f) = \left[\frac{1}{M_O^2}\right]\frac{P_{\rm RF:DUT}}{0.5\langle i_{\rm dc:DUT}^2\rangle R_L}. \tag{18}$$

In some test applications it may be preferable to measure the DUT's frequency response in terms of the coupling ratio instead of the bias current or average power. This may be the case when the DUT has poor dc stability or when the frequency response will be normalized to the response at a specific frequency (eliminating the coupling ratio). In this case, (17) and (18) can be combined to give

$$\Re_{\rm DUT}^2(f) = \frac{P_{\rm RF:DUT}}{P_{m:\rm ref}}\mathbb{R}^2(f)\beta^2 \tag{19}$$

TABLE I
SUMMARY OF TYPICAL FREQUENCY RESPONSE MEASUREMENT UNCERTAINTIES FOR PHOTODIODE WITH RF POWER SENSOR AND 3 dB ATTENUATOR

Source of uncertainty	1σ, %
Type A	
Measurement repeatability	<0.05
Type B	
Meter scaling	0.5
Meter offset	0.023
Optical power drift (power matching)	0.07
Bias current measurement	0.35
Power sensor noise, @ 0.06 GHz	0.005
@ 26 GHz	0.05
Total uncertainty	0.62
Expanded uncertainty (coverage factor = 2), %	1.2
Expanded uncertainty (coverage factor = 2), dB	0.05

where β is the ratio of the optical power coupled to the reference arm to the power coupled to the test arm.

In the case of the amplified receiver the combined response of the DUT is

$$g^2(f) = \frac{G^2(f)}{C} = \frac{2R_L P_m}{P_{\rm avg}^2} \tag{20}$$

and can be used to find the modulation depth of the source from the equation

$$M_O^2 = \frac{2R_L P_{m:\rm ref}}{g^2(f)P_{\rm avg:ref}^2}. \tag{21}$$

The DUT's response is then

$$G_{\rm DUT}^2(f) = \frac{2R_L P_{\rm RF:DUT}}{M_O^2 P_{\rm avg:DUT}^2}. \tag{22}$$

VII. UNCERTAINTY IN PHOTODIODE/POWER SENSOR COMBINED RESPONSE

Uncertainties in the measurement of a photodiode with a current monitor and a receiver without a current monitor are different. Uncertainties peculiar to the amplified receiver will be discussed in the next section. Typical uncertainties for the photodiode are listed in Table I [10]. Type A uncertainties are uncertainties which can be calculated using purely statistical analysis. Type B uncertainties are inferred by other means. The coverage factor of 2 gives 95% confidence that the true value of the frequency response lies within the interval [measured value ± expanded uncertainty] if all the uncertainties obey a Gaussian distribution. The type B uncertainties that are important for this type of transfer standard are quantities which might vary with frequency or which might change during the measurement. For example, the power meter which provides the interface circuitry to the power sensor is not considered

part of the transfer standard in this study (although it could be). Hence, range-scaling uncertainties in the meter are included in the uncertainty budget. The current monitor is also included because its offset may drift slightly. We anticipate that most customers who are interested in calibrations of this type will be mostly interested in uncertainties which might change the shape of the frequency response and are not as concerned with the absolute response. Hence uncertainties in the 50 MHz calibration standard in the power meter are not included explicitly. Optical connector repeatability is not an issue in this measurement since the response is normalized to the dc photocurrent. Power meter scaling and bias current monitor uncertainties are the dominant contributions to the uncertainty budget. Details of the uncertainty budget are given below.

1) Repeatability: Since the heterodyne system uses a swept measurement, different scans will not repeat exactly the same frequencies. The response and its standard error at the requested frequencies are found using the following method. Let $\mathbb{R}^2(f)$ be the measured response at frequency f. The calculation is usually performed with $\mathbb{R}^2(f)$ in dB with negligible error because the scatter in the data is small. The response at the requested frequency x is estimated by a kernel-type smoother [11]. Specifically

$$\tilde{\mathbb{R}}^2(x) = \frac{\sum_{i=1}^{n} K\left(\frac{x-f_i}{b}\right)\mathbb{R}^2(f_i)}{\sum_{i=1}^{n} K\left(\frac{x-f_i}{b}\right)} \tag{23}$$

where b is the bandwidth parameter and $K(\cdot)$ is the kernel function, which typically has the following properties:

$$\begin{aligned} &1)\quad K(\xi) \geq 0 \quad \text{for all } t \\ &2)\quad \int_{-\infty}^{\infty} K(\xi)\, d\xi = 1 \\ &3)\quad K(-\xi) = K(\xi) \quad \text{for all } \xi. \end{aligned} \tag{24}$$

That is, $\tilde{\mathbb{R}}^2(x)$ is obtained as a weighted average of frequency responses around x. The kernel function assigns the weight to each point, and the bandwidth b determines the size of the region around x for which $\mathbb{R}^2(f_i)$ receives relatively large weights. Frequently used kernels include rectangle, triangle, and Gaussian functions. The rectangular kernel assigns equal weight to the points inside the rectangle and ignores the points outside. Both the triangle and Gaussian kernel assign the most weight to the points that are closer to x. In our applications, we use the Gaussian kernel

$$K(\xi) = \frac{1}{0.37\sqrt{2\pi}} e^{-\xi^2/2(0.37)^2} \tag{25}$$

The kernel is scaled to have 25th percentile of -0.25 and a 75th percentile of 0.25. Many methods have been proposed for bandwidth selection [12]. In practice, b can be determined by the average frequency increment in the scan, and the desired number of points used to calculate $\tilde{\mathbb{R}}^2(x)$. For example, if the Gaussian kernel is used, the average frequency increment is h, and roughly p points on each side of x are to be included; that is $|x - f_i| \leq ph$. Any point with $|(x - f_i)/b| > 1$ receives almost 0 weight; that is, we want $|(x - f_i)/b| \leq 1$ or $b \approx ph$. The "resolution" of the measurement is then about $0.37ph$. We typically take data so that the spacing between acquired points is 0.1 to 0.2 times the final data spacing (resolution) required. We then use $p = 2$ giving an approximate resolution of 0.07 to 0.14 times the required data spacing.

The kernel smoothing technique, like all other smoothing techniques, has an error associated with it. This error is small when the data are roughly linear with frequency, but may become significant in regions with large curvature. The approximate mean-square error of the kernel estimator $\tilde{\mathbb{R}}^2(x)$ is given by [13]

$$\mathrm{MSE}\,(x) = 0.004\,685 b^4 c_x^2 + \frac{0.762\,42\sigma_x^2}{nb} \tag{26}$$

where c_x is the second derivative of $\mathbb{R}^2(y)$ evaluated at $y = x$ and σ_x^2 is the variance of the response at frequency x. This variance, however, is unknown and needs to be estimated. A technique [14] which works well and can be used to obtain an estimate of σ_x^2 is to "detrend" the data locally and use the sample variance of the detrended data. The "detrended" residual value at f_i is defined as

$$r_i = \mathbb{R}^2(f_i) - \frac{\mathbb{R}^2(f_{i+1}) + \mathbb{R}^2(f_{i-1})}{2} \tag{27}$$

and the variance estimator is found by

$$\hat{\sigma}_x^2 = \frac{2}{3(n-2)} \sum_{i=2}^{n-1} r_i^2. \tag{28}$$

Let $\tilde{\mathbb{R}}_i^2(x)$ and $\mathrm{MSE}_i(x)$ be the estimated response and the mean square error at frequency x of the ith scan. The estimated mean response based on m scans is

$$\overline{\tilde{\mathbb{R}}^2}(x) = \sum_{i=1}^{m} \frac{\tilde{\mathbb{R}}_i^2(x)}{m} \tag{29}$$

and its standard error is

$$s(x) = \sqrt{\frac{s_b^2(x) + s_w^2(x)}{m}} \tag{30}$$

where

$$s_b(x) = \sqrt{\sum_{i=1}^{m} \frac{(\tilde{\mathbb{R}}_i^2(x) - \overline{\tilde{\mathbb{R}}^2}(x))^2}{m-1}} \tag{31}$$

is the between-scan uncertainty and

$$s_w^2(x) = \sum_{i=1}^{m} \frac{\mathrm{MSE}_i(x)}{m} \tag{32}$$

is the uncertainty within a scan due to the kernel smoothing process.

Repeatability is a function of the connector type, frequency, mismatch, and other factors which cannot be controlled. Other smoothing techniques can also be used, in particular, the spline methods. We did not use a spline method to interpolate the measurements because spline methods give unsatisfactory results near the end points, use arbitrary knot spacing, and

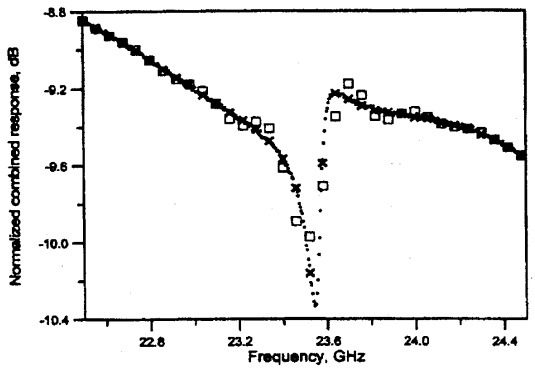

Fig. 3. Dots represent the measured responses, □ denotes the interpolated responses at requested frequencies based on a cubic spline fit, and × and denotes the Gaussian kernel smoother.

give a poorly defined resolution. In addition, the splines over smooth the "peaks" and "valleys." For example, the dots in Fig. 3 represent the measured response, □ denotes the interpolated responses at requested frequencies based on a cubic spline fit, and × denotes the interpolated responses at requested frequencies based on the Gaussian kernel smoother. In most cases, both methods agree well, but clearly the spline method gives poorer results in the neighborhood of 23.5 GHz. Uncertainty due to the kernel smoothing is negligible on most detectors which we have calibrated, for example, $s_w \leq 0.002$ dB for the data in Fig. 3.

2) Meter Scaling: The absolute accuracy of the power meter is specified by the manufacturer as 0.5% and is assumed to be 1σ. This is conservative; if the specified uncertainty was actually 2σ the calibration uncertainty would be reduced.

3) Meter Offset: The settability of the zero level, specified as one least significant count on the display or 0.001 dB or 0.023%, is assumed to be 1σ.

4) Optical Power Drift (Power Matching): Power from one or both of the lasers which is coupled into the fiber may drift during the measurement. Also because of the long coherence length of the Nd:YAG laser, etalon effects cause the power matching between the two lasers to vary with frequency. The power from each laser does not drift by more than 4%, giving a 0.05% uncertainty in the ratio of (4). This quantity is considered 1σ for one of the lasers.

5) Bias Current Measurement: The scale factor in the current monitor used in this study had a temperature coefficient of 0.14%/°C. The laboratory has about ±2.5 °C worst case drift.

6) Power Sensor Noise: This is the uncertainty associated with the background RF noise of the detector, which is about −80 dB (1 mW) for the diode power sensor. The background noise is about −40 dB (1 mW) for the thermal power sensor.

VIII. Uncertainties of Amplified Receiver/Power Sensor Combined Response

Typical uncertainties for the receiver are listed in Table II [10]. Dominant uncertainties are fiber connector insertion loss, power meter scaling, coupling ratio measurement, and power

TABLE II
Summary of Typical Frequency Response Measurement Uncertainties for the Amplified Photoreceiver with Thermal RF Power Sensor

Source of uncertainty	1σ, %
Type A	
Measurement repeatability, @ 10 MHz	0.05
@ 1500 MHz	1.1
Type B	
Meter scaling	0.5
Meter offset	0.023
Coupling ratio	0.35
Optical power drift (power matching)	0.07
Receiver linearity, estimated from proto 900	0.1
Power sensor noise, @ 10 MHz	0.2
@ 1500 MHz	3.8
Total uncertainty, @ 10 MHz	0.66
@ 1500 MHz	4.0
Expanded uncertainty (coverage factor = 2), @ 10 MHz	1.3
@ 1500 MHz	8.0
Expanded uncertainty (coverage factor = 2), dB @ 10 MHz	0.06
@ 1500 MHz	0.34

sensor noise. Correction for the fiber connector insertion loss must be included to reduce uncertainty to an acceptable level.

1) Coupling Ratio: The coupling ratio is measured at the beginning of a measurement and then the 10% port is monitored during the scan to infer the power reaching the receiver. The fiber-to-air launch from the coupler monitor port into the power meter is terminated with a connector angled at 8° to minimize coherent multiple path effects. Coherent effects due to nonzero return loss (typically 30 dB) give repeatable systematic uncertainties of about 0.35% (1σ). Coupling ratio drift during the scan is random and is included in the repeatability described above.

2) Offset Correction: When the frequency response is normalized to the optical power (instead of photocurrent) a further uncertainty is the repeatability of connecting fibers to the DUT and to the optical power meter for calibration of the coupler. This effect is a constant scale factor (offset on a logarithmic scale) for each scan and does not have a frequency dependence (provided that coherent multipath effects are insignificant). The fiber connector insertion loss repeatability is typically about 0.1 dB and is larger than other uncertainties in the measurement. Also, scans over the low and high frequency ranges were made separately and with different data spacing, so a method for "splicing" the two overlapping frequency ranges together is required. This is accomplished by shifting all the scans to a common level (on a logarithmic scale) selected by a least-median technique. Using this technique, the individual scans are shifted by averaging over all desired frequencies where scans overlap. The absolute response then has a relatively large uncertainty, while the shape is specified to much lower uncertainties. The technique described below

for logarithmic data does not apply for offsets or outliers larger than a few tenths of a decibel.

If there are m scans over frequencies f_i, then offset adjustment factors a_j can be calculated by minimizing the expression

$$\sum_{i=1}^{n} d(\tilde{\gamma}_1(f_i) - a_1, \tilde{\gamma}_2(f_i) - a_2, \cdots, \tilde{\gamma}_m(f_i) - a_m) \quad (33)$$

where $d(\cdot, \cdot, \cdots, \cdot)$ is an "appropriate" distance metric and $\gamma = 20\log(g)$. A possible metric for our application is absolute deviation from the mean. Let

$$\overline{\gamma}(f_i) = \sum_{j=1}^{m} \frac{\tilde{\gamma}_j(f_i)}{m} \quad (34)$$

be the mean response at f_i and define the distance metric as the sum of the distance (absolute difference) between $\tilde{\gamma}_j(f_i) - a_j$ and $\overline{\gamma}(f_i)$ the mean response

$$d(\tilde{\gamma}_1(f_i) - a_1, \cdots, \tilde{\gamma}_m(f_i) - a_m) = \sum_{j=1}^{m} |\tilde{\gamma}_j(f_i) - a_j - \overline{\gamma}(f_i)|. \quad (35)$$

The expression we need to minimize is

$$\sum_{j=1}^{m}\sum_{i=1}^{n} |\tilde{\gamma}_j(f_i) - a_j - \overline{\gamma}(f_i)|. \quad (36)$$

Given the sequence $y_1, y_2, \cdots, y_n$ the value of a that minimizes

$$\sum_{i=1}^{n} |y_i - a| \quad (37)$$

is a = median of $y_1, y_2, \cdots, y_n$. Thus the solution for a_j is that a_j is the median of

$$\tilde{\gamma}_j(f_1) - \overline{\gamma}(f_1), \tilde{\gamma}_j(f_2) - \overline{\gamma}(f_2), \cdots, \tilde{\gamma}_j(f_n) - \overline{\gamma}(f_n). \quad (38)$$

The fiber connector repeatability and its associated offset can be characterized by the standard deviation of the a_j but is not considered an uncertainty in the transfer standard. The repeatability at a given frequency is then found using the offset adjusted data in (30).

3) Receiver Linearity: The receiver saturates with input at about −5 dB (1 mW). Since the power detection is not frequency selective, harmonics of the modulated signal due to nonlinearity give an error in the power reading. To characterize the receiver nonlinearity around a few megahertz, the optical power was varied and harmonics were measured on an electrical spectrum analyzer. An optimum average optical power input is about −10 dB (1 mW) to −13 dB (1 mW), which is a compromise between receiver nonlinearity and power sensor noise. Uncertainty due to nonlinearities is typically less than 0.1% at this power.

4) Receiver Stability: Measurements at frequencies well above the receivers cut off show additional instability. We think this is related to the low open loop gain of the receiver amplifier at these frequencies (see repeatability at 1500 MHz in Table II).

5) Receiver Noise: Some broadband receivers generate noise signals significantly higher than the power sensor noise floor, giving poor dynamic range in the heterodyne measurements. We have found that the noise power is fairly stable and can be subtracted from the measured power in the heterodyne system, giving significant improvements in the measurement dynamic range. This was not necessary for the receiver described in this paper.

IX. Sources of Uncertainty in Ratio Measurement System

The following is a brief list of error sources which must be considered when designing a ratio test system.

1) Type of DUT: Equations (18), (19), and (22) include the RF power measured from the DUT. If the DUT is a photodiode or photoreceiver, the power must be measured with some kind of electrical transducer which will indicate how much electrical power is being generated. The calibration factor and impedance mismatch of this transducer must also be included in the customers error budget. However, if the DUT is a device which includes the transducer, such as a lightwave communications analyzer or lightwave spectrum analyzer, the frequency response of the device as a whole is measured, eliminating calibration factor and mismatch uncertainty.

2) Spurious Harmonics: Harmonics due to nonlinearities in directly modulated lasers or over driving and inaccurate bias of external modulators can cause some harmonic content [15]. The RF signal generator can also be a source of spurious harmonic and nonharmonic signals. Since the RF power sensor is not frequency selective, energy at spurious frequencies gives a systematic error. Assuming that the power sensor acts as a true rms detector, the powers add arithmetically. To keep the increase in uncertainty below 10%, the total harmonic power must be greater than 22 dB lower than the fundamental. Errors due to harmonics can also be corrected using iterative techniques.

3) Relative Intensity Noise: Again energy at frequencies other than the modulation frequency can give systematic errors. The effect of RIN can be estimated by measuring the noise level from the transfer standard when the optical source is not modulated. Errors due to relative intensity noise can be corrected using iterative techniques.

4) Wavelength Dependence: Wavelength dependence of a photodiode is a complicated function of the depletion region thickness, intrinsic layer thickness, bias voltage, and other parameters. It can be as much as several tenths of a decibel [5]. This effect can be minimized by operating the ratio test system at the same wavelength as the original calibration or corrections can be performed if the transfer standard can be accurately modeled.

X. Results

A typical measurement of the combined normalized response of a photodiode/attenuator/power sensor transfer standard is shown in Fig. 4 along with the expanded uncertainty. Data points might be required, for example, between 0.060 and 26.490 GHz in 0.060 GHz increments. The total average

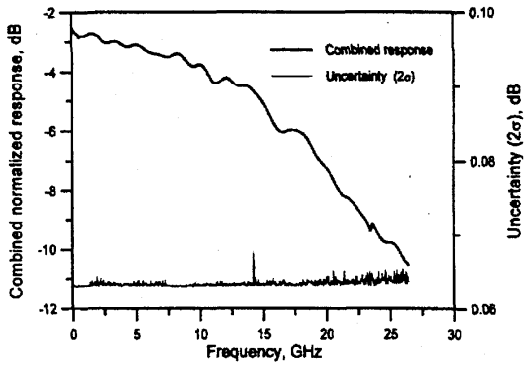

Fig. 4. Combined response and expanded uncertainty of 20 GHz photodiode/power sensor transfer standard. The small spike in the uncertainty near 14 GHz is due to an outlier in the data set which was intentionally not removed.

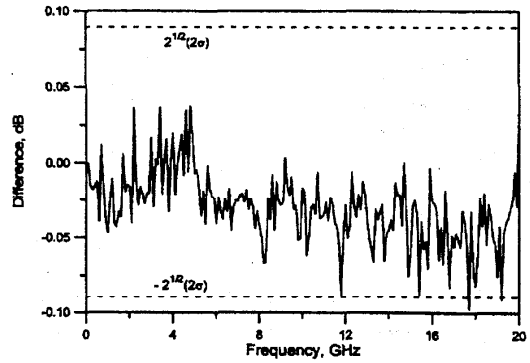

Fig. 5. Measurement of a photodiode/3 dB attenuator/RF power sensor transfer standard against a second transfer standard of the same type compared with NIST calibration. Uncertainties due to transfer standards alone are also shown.

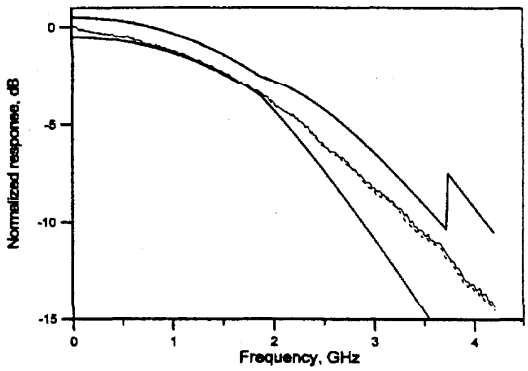

Fig. 6. Measurement of lightwave communications analyzer plug-in module with STM-16/OC-48 filter on two different ratio measurement systems, using the same two photodiode/3 dB attenuator/RF power sensor transfer standards as in the experiment shown in Fig. 5. Tolerances given in ITU-TS G.957 are also shown as thick lines.

photocurrent was 100 μA, and the low frequency RF power was about −38 dB (1 mW). Three swept scans were made with data points spaced by about 4 MHz with a delay of about 0.2 s between the step to the temperature controller on the laser and the data acquisition. Two additional scans were made from 0.5 GHz through dc and on to 0.5 GHz using a different band on the microwave counter. These scans captured points which could not be acquired using the upper frequency band.

To show that measurements using the heterodyne system are reproducible, a measurement system based on Fig. 2 was built and used to measure a transfer standard against a second transfer standard, both calibrated at NIST. The difference in the measurements is shown in Fig. 5 along with $\sqrt{2}(2\sigma)$ where 2σ is the expanded uncertainty of one transfer standard calibration as calculated in Table I averaged over the entire frequency range. The comparison falls well within the expected bounds, with insignificant uncertainty added by the ratio measurement system.

To further verify that a calibration can be transferred with acceptable accuracy, a second system based on Fig. 2 was built, using the second transfer standard. A lightwave communications analyzer plug-in module, used for testing STM-16/OC-48 eye diagrams, was measured on both systems. Each system used a different communications analyzer mainframe which was triggered by the 10 MHz reference oscillator from the system synthesized signal generator. The entire scan used a single gain setting on the mainframe. The modules measured response was normalized so that the curves just fit inside the tolerance window specified by ITU-TS G.957 (see Fig. 6). The curves agree well within the G.957 specification. The response curves also agree well within the expected combined uncertainty of the two transfer standards below 2.5 GHz. Above 2.5 GHz the difference slowly drifts up, reaching 0.2 dB above 4 GHz. The difference between the two curves also has larger scatter above 2.5 GHz. This discrepancy above 2.5 GHz is attributed to slowly degrading trigger and lower signal at high frequencies. The communications analyzer was triggered directly from the system synthesizer's 10 MHz reference oscillator, giving poor timing jitter at high frequencies [16]. This jitter might be improved by using an external trigger which operates up to 18 GHz or running the oscilloscope untriggered. As the signal decreased at high frequencies the 8 b display resolution may also cause the standard deviation to increase.

An amplified receiver/power sensor transfer standard was also measured. Data points were required in 1 MHz increments between 1 and 700 MHz and in 10 MHz increments between 710 and 1700 MHz. Three scans were taken from >700 MHz through 0 and then three in the reverse direction. Data were taken in about 1 s intervals and about 0.2 MHz data spacing. Three scans were also taken from >1700 to around 450 MHz and three in the reverse direction. Sampling for these scans was done in 5 s intervals and about 1 MHz data spacing. Data for this receiver were acquired at a lower rate than for the photodiode because of the slow thermal response of the RF power sensor. This effect is particularly important above 800 MHz where receiver response is changing rapidly. Scan rates were chosen empirically by minimizing hysteresis at the peak near 800 MHz. Average optical power delivered to the receiver was −10 dB (1 mW), giving about −12.5 dB (1 mW) RF power. The scans of the combined response of the amplified receiver/power sensor before offset correction

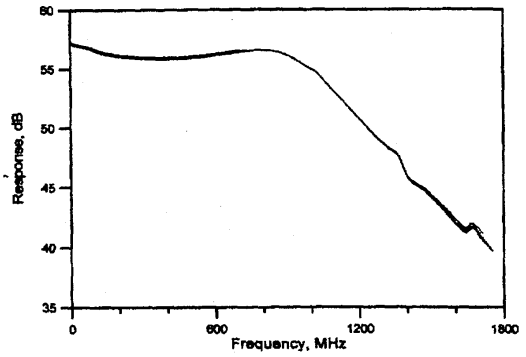

Fig. 7. Measured combined response of amplified receiver/power sensor transfer standard before correction for fiber connector insertion loss. Graph shows seven scans.

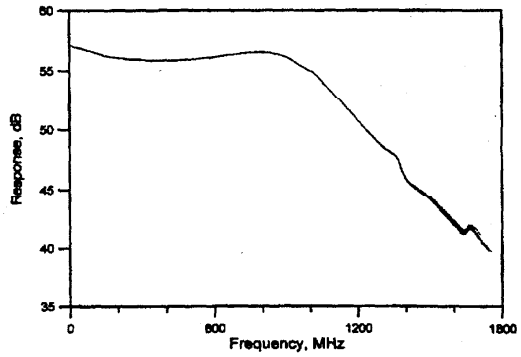

Fig. 8. Measured combined response of amplified receiver/power sensor transfer after correction for fiber connector insertion loss.

are shown in Fig. 7 and after offset correction in Fig. 8. The standard deviation of the a_i for the level shifts was 0.05 dB.

To show that a calibration could be transferred accurately, he frequency response of a lightwave communications analyzer (which is used for STM-1/OC-3 eye diagram testing according to ITU-TS SDH/SONET specification G.957 [1]) was measured using two different transfer standard amplified receiver/power sensor units. Measurements were made between 1 and 620 MHz at 51 points. Results were normalized to the lowest-frequency point (1 MHz). The difference between the two measurements is shown in Fig. 9 along with $\sqrt{2}(2\sigma)$ where 2σ is the total expanded uncertainty of one transfer standard calibration as calculated in Table II averaged over the entire frequency range. The mean difference is -0.02 dB with a standard deviation of 0.044 dB. The slight systematic offset may be due to the fact that the curves were normalized to the lowest-frequency point, which has a slightly larger uncertainty than frequencies a few megahertz higher. The apparent trend upward toward higher frequencies is not statistically significant. Although the expanded uncertainty for the transfer standards is 0.06 dB; the only uncertainties which show up in this comparison are random (type A). The random component of the transfer standard is about 0.1%, and the two-cursor uncertainty in the oscilloscope is limited by the

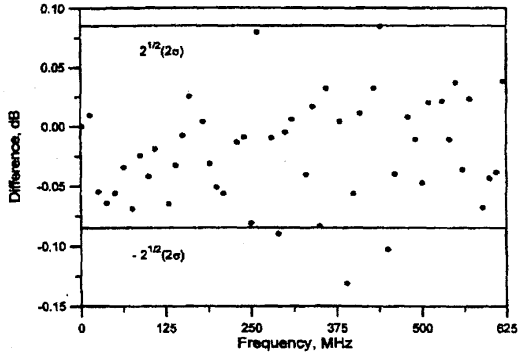

Fig. 9. Difference in measured response of lightwave communications analyzers with STM-1/OC-3 filter using two different amplified receiver/power sensor transfer standards. Uncertainty due to transfer standards alone are also shown.

8 b A/D resolution giving an uncertainty of 0.4%. The total random uncertainty for the measurement is then 0.6% or 0.05 dB, in good agreement with the measured result.

XI. Conclusions

Our heterodyne measurement system can be used to calibrate photoreceiver frequency response transfer standards with uncertainty less than ± 0.06 dB (coverage factor = 2). This is a factor of 5 smaller than the smallest tolerance required by ITU-TS G.957 for SDH/SONET reference receivers for measuring eye diagrams. The low uncertainty is attained by combining a photoreceiver with a RF power sensor in one transfer standard, eliminating uncertainties due to power sensor calibration and impedance mismatch. We have also shown that the calibration can be transferred to a ratio measurement system suitable for a manufacturing environment. The source used in the ratio system may have an arbitrary modulation depth. Transfer standards calibrated at NIST and measured on a ratio system agreed well within the calibration uncertainties.

Acknowledgment

The authors would like to thank M. McClendon, Hewlett-Packard, Santa Rosa, CA, for facilitating the interactions between NIST and Hewlett-Packard and for many useful discussions. They would also like to thank J. Juroshek, NIST, Boulder, CO, for useful discussions on microwave metrology and M. Young, NIST, Boulder, CO, for editorial comments.

References

[1] Contribution of National Institute of Standards and Technology, not subject to copyright.

[2] Optical interfaces for equipments and systems relating to the synchronous digital hierarchy, CCITT (now ITU-TS) recommendation G.957, Geneva, Switzerland, 1990.

[3] In this work, all ratios are stated in decibels electrical, that is, $20 \log (A2/A1)$ where A is a voltage or current. Absolute powers are stated with the reference level, such as -10 dB (1 mW) instead of -10 dBm as suggested in Letter symbols to be used in electrical technology, Part 3: Logarithmic quantities and units, IEC 27-3, Geneva, Switzerland, 1989.

[4] J. A. Valdmanis and J. V. Rudd, "High-speed optical signals demand quick response," *Laser Focus World*, pp. 141–147, Mar. 1995.

[5] D. A. Humphreys, T. Lynch, D. Wake, D. Parker, C. A. Park, S. Kawanishi, M. McClendon, P. Hernday, J. Schlafer, A. H. Gnauck, G. Raybon, R. T. Hawkins II, M. D. Jones, and J. H. Goll, "Summary of results from an international high-speed photodiode bandwidth measurement intercomparison," in *Digest Optic. Fiber Measurements Conf.*, York, U.K., pp. 69–72, 1991.
[6] A. D. Gifford, D. A. Humphreys, and P. D. Hale, "Comparison of photodiode frequency response measurements to 40 GHz between NPL and NIST," *Electron. Lett.*, vol. 31, pp. 397–398, 1995.
[7] Fundamentals of RF and microwave power measurements, Hewlett-Packard Application Note 64-1, 1978.
[8] B. Wong and H. Kosiorska, "Factory measurement solutions to predictable field performance of single mode fiber optic connectors," Nat. Inst. Stand. Technol. Spec. Pub. 839, Tech. Digest-Symp. Optical Fiber Measurements, 1992, G. W. Day and D. L. Franzen, Eds., 1992, pp. 23–28.
[9] R. L. Gallawa and X. Li, "Calibration of optical fiber power meters: The effect of connectors," *Appl. Opt.*, vol. 26, pp. 1170–1174, 1987.
[10] Guidelines to the expression of uncertainty in measurement, ISO, Geneva, Switzerland, 1993.
[11] B. W. Silverman, Density estimation for statistics and data analysis. London, England: Chapman and Hall, 1986, pp. 34–72.
[12] W. Hädle, *Smoothing Techniques With Implementation in Statistics*. New York: Springer-Verlag, 1991.
[13] N. S. Altman, "An introduction to kernel and nearest-neighbor nonparametric regression," *The Amer. Statistician*, vol. 46, pp. 175–185, 1992.
[14] J. Rice, "Bandwidth choice for nonparametric regression," *The Ann. Statist.*, vol. 12, pp. 1215–1230, 1984.
[15] P. D. Hale, D. A. Humphreys, and A. D. Gifford, "Photodetector frequency response measurements at NIST, US, and NPL, UK: Preliminary results of a standards laboratory comparison," in *Proc. Soc. Photo-Optical Instrum. Eng.* vol. 2149, 1994, pp. 345–355.
[16] D. Henderson and A. G. Roddie, "A comparison of spectral and temporal techniques for the measurement of timing jitter and their application in a modelocked argon ion and dye laser system," *Opt. Commun.*, vol. 100, pp. 456–460, 1993.

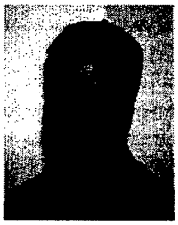

Paul D. Hale received the Ph.D. degree in applied physics from the Colorado School of Mines, Golden, in 1989.

He has worked with the Optoelectronics Division of NIST, Boulder, CO, since 1984. He has conducted research in birefringent devices, modelocked fiber lasers, fiber chromatic dispersion, broadband lasers, interferometry, polarization standars, and photodiode frequency response. He is presently leader of the High Speed Measurements Project in the Sources and Detectors Group.

Dr. Hale received the Department of Commerce Gold Medal along with a team of four other scientists for measuring fiber cladding diameter with an uncertainty of 30 nm in 1994.

C. M. Wang received the Ph.D. degree in statistics from Colorado State University, Fort Collins in 1978.

He is a mathematical statistician in the Statistical Engineering Division, National Institute of Standards and Technology, Boulder, CO. His research concentrates on linear models, variance components, uncertainty analysis, and statistical computing.

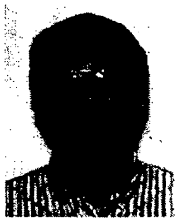

Rin Park was born in Pohang, Korea. He graduated from California State Polytech, Pomona in 1983.

He joined Hewlett–Packard, Network Measurement Division (NMD), Santa Rosa, CA, as a Manufacturing Design Engineer in 1983. He designed a 50 GHz vector network analyzer system that involved both coax and two waveguide test sets before Hewlett–Packard came up with all coax 50 GHz vector network analyzer. He joined the Signal Analysis Division R&D, Santa Rosa, CA, where he designed RF circuits and log amps. He joined the Manufacturing Department of Lightwave Operation, Santa Rosa, 1993. He designed the optical communication analyzer test system with the help of Dr. P. D. Hale at NIST.

Wai Yuen Lau received the B.S.E.E. degree from the University of California at Santa Barbara and the B.A. degree in business management from Sonoma State University, Rohnert Park, CA.

In 1978, he joined Hewlett–Packard Company (HP). Currently, he serves as a Systems Hardware Development Engineer with HP, Santa Rosa, CA, Systems Division where he develops and defines the HP 84000 RFIC Test System specifications. In the past, he has served as a Manufacturing Development Engineer with HP Lightwave Operation. He has also worked on the HP 83475 Digital Communication Analyzer as well as the HP 83440 and 83441/2 series of optical-to-electrical detectors. His main responsibility was to develop new production test strategies and product specification. His other HP project assignments have included analyzing and enhancing the HP 85150 microwave and RF design system's software linear simulation models and developing production tests and test equipment for the HP 8510 Network Analyzer microcircuit assemblies.